THE JOURNAL OF BIOLOGICAL CHEMISTRY VOL. 281, NO. 21, pp. 14644–14653, May 26, 2006

Distinct Glycan Structures of Uroplakins Ia and Ib

*STRUCTURAL BASIS FOR THE SELECTIVE BINDING OF FimH ADHESIN TO UROPLAKIN Ia**[S]

Received for publication, January 27, 2006, and in revised form, March 21, 2006 Published, JBC Papers in Press, March 27, 2006, DOI 10.1074/jbc.M600877200

Bo Xie[‡1], Ge Zhou[§1], Shiu-Yung Chan[‡], Ellen Shapiro[¶], Xiang-Peng Kong[‖], Xue-Ru Wu[¶], Tung-Tien Sun[§¶‡‡2], and Catherine E. Costello[‡2]**

*From the [‡]Mass Spectrometry Resource, Boston University School of Medicine, Boston, Massachusetts 02118 and Departments of [§]Dermatology, [¶]Urology, [‖]Biochemistry, **Microbiology, and [‡‡]Pharmacology, New York University School of Medicine, New York, New York 10016*

Although it has been shown that mouse uroplakin (UP) Ia, a major glycoprotein of urothelial apical surface, can serve as the receptor for the FimH lectin adhesin of type 1-fimbriated *Escherichia coli*, the organism that causes a great majority of urinary tract infections, the glycan structure of this native receptor was unknown. Using a sensitive approach that combines in-gel glycosidase and protease digestions, permethylation of released glycans, and mass spectrometry, we have elucidated for the first time the native glycoform structures of the mouse UPIa receptor and those of its non-binding homolog, UPIb, and have determined the glycosylation site occupancy. UPIa presents a high level of terminally exposed mannose residues (located on $Man_6GlcNAc_2$ to $Man_9GlcNAc_2$) that are capable of specifically interacting with FimH. We have shown that this property is conserved not only in the mouse uroplakins but also in cattle and, even more importantly, in human UPIa, thus establishing the concept that UPIa is a major urothelial receptor in humans and other mammals for the mannose-specific FimH variant. In contrast, our results indicate that most terminally exposed glycans of mouse UPIb are non-mannose residues, thus explaining the failure of FimH to bind to this UPIb. In cattle, on the other hand, complex carbohydrates constituted only about 20% of the UPIb *N*-linked glycans. Human UPIa contained exclusively high mannose glycans, and human UPIb contained only complex glycans. The drastically different carbohydrate processing of the UPIa and UPIb proteins, two closely related members of the tetraspanin family, may reflect differences in their folding and masking due to their interactions with their associated proteins, UPII and UPIIIa, respectively. Results from this study shed light on the molecular pathogenesis of urinary tract infections and may aid in the design of glyco-mimetic inhibitors for preventing and treating this disease.

The essential first step in mucosal infection is for the microorganisms to latch onto the mucosal surfaces to escape being expelled by physical forces and other innate host defenses (1). Indeed, many microorganisms are equipped with sophisticated devices that allow them to adhere to and colonize a particular mucosal niche and cause organ-specific infections. The type 1-fimbria, a slender filamentous appendage made by almost all uropathogenic *Escherichia coli*, is such a device and is obligatory for *E. coli* adhesion to the urothelial surface (2–4). The fimbriae are made up of four protein components (FimA, -F, -G, and -H), with homo-polymeric FimA forming a long, cylindrical shaft projecting outward from the *E. coli* and a single FimH adhesin strategically located at the distal tip of each fimbria (5–7). A crystallographic study revealed that the FimH subunit consists of two distinct domains, an N-terminal lectin domain encircling a carbohydrate binding pocket and a C-terminal pilin domain (8, 9). This structural model predicts that the binding pocket of FimH is capable of accommodating a single mannose residue, a finding highly consistent with earlier *in vitro* studies where type 1-fimbriated *E. coli* can efficiently agglutinate mono-mannose-bearing latex beads as well as erythrocytes and bakers' yeast, both known to express high mannose surface glycoproteins (10). However, mono-mannose proteins do not exist in nature, and erythrocytes and yeast are not involved in *E. coli* adhesion to the urothelial surface. Critical information is lacking, therefore, regarding the detailed carbohydrate structure of the urothelial receptor that is physiologically responsible for binding the FimH lectin adhesin.

The urothelial surface is almost completely occupied by 16-nm protein particles hexagonally packed into two-dimensional crystals called asymmetric unit membrane (AUM)[3] or urothelial plaques (11–15). Each particle can be further divided into a six-subdomain inner ring and six-subdomain outer ring (12–14, 16–18). The particles are now known to be composed of four major proteins, termed uroplakin Ia (UPIa; 27 kDa), UPIb (29 kDa), UPII (15 kDa), and UPIIIa (47 kDa) (19–24). UPIa and UPIb each contain four transmembrane domains and interact with single transmembrane-domain partners, UPII and UPIIIa, respectively (15, 25, 26). Whereas the mature form of UPII is not glycosylated, UPIa, -Ib, and -IIIa are all modified with *N*-linked glycans, as evidenced by electrophoretic mobility reduction after *N*-glycosidase digestions (20, 22, 23). The sheer abundance of the uroplakins on the urothelial surface and the fact that some of them carry *N*-linked glycans raised the interesting possibility that one or more of the uroplakins may serve as the urothelial receptor(s) for FimH lectin adhesin. This hypothesis has been proven correct by several independent *in vitro* and *in vivo* studies. First, type 1-fimbriated, but not P-fimbriated or non-fimbriated, *E. coli* bound to highly purified bovine AUM containing primarily the four uroplakins (27). A gel overlay assay using radiolabeled, type 1-fimbriated *E. coli* revealed that bovine UPIa and -Ib, both sensitive to endoglycosidase H (Endo H) treatment, bound to the *E. coli*. Nei-

* This work was supported by National Institutes of Health Grants P41 RR10888 and S10 RR15942 (to C. E. C.), R01 DK39753 (to T.-T. S.), and P01 DK52206 (to X.-P. K., X.-R. W. and T.-T. S.). The costs of publication of this article were defrayed in part by the payment of page charges. This article must therefore be hereby marked "*advertisement*" in accordance with 18 U.S.C. Section 1734 solely to indicate this fact.

[S] The on-line version of this article (available at http://www.jbc.org) contains supplemental Figs. 1–6.

[1] These authors have made equal contributions.

[2] To whom reprint requests and correspondence should be addressed: Mass Spectrometry Resource, Departments of Biochemistry and Biophysics, Boston University School of Medicine, 670 Albany St., Rm. 511, Boston, MA 02118. Tel.: 617-638-6490; Fax: 617-638-6491; E-mail: cecmsms@bu.edu.

[3] The abbreviations used are: AUM, asymmetric unit membrane; UP, uroplakin; Endo H, endoglycosidase H; PNGase F, peptide *N*-glycosidase F; MALDI-TOF MS, matrix-assisted laser desorption/ionization time-of-flight mass spectrometry; ESI, electrospray ionization.

ther non-glycosylated UPII nor highly glycosylated UPIIIa (sensitive only to peptide *N*-glycosidase F (PNGase F) treatment) showed any binding, strongly indicating a high degree of ligand-receptor specificity (27). Second, under quick-freeze, deep-etch microscopy in a mouse ascending urinary tract infection model, the tips of type 1-fimbriae were seen to make direct contact with the central depression surrounded by the inner ring within the 16-nm uroplakin particle (28). This study provided the first *in vivo* evidence indicating that the uroplakins can serve as the physiological receptors for the FimH adhesin. FimH-mediated binding to urothelial surface can also trigger urothelial cells to engulf the bacteria, thus insulating the pathogen from host defenses (29, 30). Third, electron microscopy-based domain mapping studies using recombinant FimH as a probe localized the FimH binding sites to the inner 6 subdomains of the 16-nm protein particles (31). Finally, naturally occurring phenotypic variants of FimH showed different binding affinities to highly purified AUMs. Those *E. coli* that exhibit high affinity binding to the mono-mannose moieties and that are primarily found in urinary tract infection isolates bind to purified AUMs in much greater numbers than those binding only to the tri-mannose structures that have been identified mainly in the fecal isolates (32). Together, these data strongly suggest that uroplakins play critical roles not only in mediating *E. coli* adhesion and internalization but also in providing a selective advantage for certain types of *E. coli* strains to preferentially colonize the urinary tract.

Despite these advances, several critically important questions have remained unanswered. For instance, in mice, whose UPIa and -Ib can easily be resolved on SDS-PAGE, we have reported that FimH bound preferentially to UPIa, despite the fact that a significant portion of mouse UPIb is sensitive to Endo H, which is known to release "high mannose" glycans (33). An even more important and clinically relevant question is whether human UPIa, like that of its mouse counterpart, can also serve as the receptor for FimH. In addition to these unsettling issues, the structural basis for FimH so reproducibly binding UPIa has not been determined. It seemed clear that elucidating the detailed oligosaccharide structures of both UPIa and -Ib from different species in conjunction with FimH binding studies should help resolve many of these important issues.

Because of the difficulty in individually isolating the highly insoluble uroplakins and because of the complexity and heterogeneity of the carbohydrates, it has been a technical challenge to determine the oligosaccharide structures of the uroplakins to enable establishing the structure-function relationships (34–37). In this study we utilized the sophisticated and sensitive approach of mass spectrometry combined with in-gel glycosidase digestions followed by microscale permethylation of released glycans and tandem mass spectrometry to accomplish detailed analyses of the *N*-linked glycans present in UPIa and -Ib of mouse and cattle. Despite the small quantities available and the great complexity typically present in biological samples, we demonstrate that this approach can quickly provide abundant structural and quantitative information. We also mapped the locations of the *N*-glycosylation sites that actually harbor glycans in both proteins through subsequent in-gel protease digestion of the deglycosylated proteins and mass spectral sequencing of the proteolytic peptides. Finally, we provide critical evidence that human UPIa, but not UPIb, has Endo H-sensitive (high mannose) glycans and can bind FimH. Results from these studies provide a molecular explanation as to why UPIa and UPIb bind FimH differently and shed light on the roles of different uroplakins in the pathogenesis of urinary tract infections.

EXPERIMENTAL PROCEDURES

Reagents—The chemicals and their sources are listed below. Enzymes including recombinant, glycerol-free PNGase F, Endo H (New England Biolabs Inc, Beverly, MA), and trypsin (Promega Corp., San Luis Obispo, CA) were used in digestions. The matrix-assisted laser desorption/ionization reflectron time-of-flight mass spectrometer (MALDI MS) matrices 2,5-dihydroxybenzoic acid and α-cyano-4-hydroxycinnamic acid (Bruker, Billerica, MA), the permethylation reagents dimethyl sulfoxide, sodium hydroxide, and methyl iodide as well as chloroform and other solvents (Sigma-Aldrich) were stored under dry conditions. Recombinant FimH/C complex was produced as described previously (38).

Isolation of Urothelial Plaques—Urinary bladders from murine and bovine species were obtained within 4 h postmortem. Human urothelial cells were collected from 14–16-week-old embryonic bladders. The acquisition and use of human tissues and the donor consent form have been approved by the Institutional Review Board of NYU Medical School. Urothelial plaques were isolated by sucrose density gradient centrifugation coupled with differential detergent washes (21). The resulting urothelial plaque proteins were solubilized in 1% SDS and quantitated using the BCA reagent.

FimH Overlay Assay—Proteins in the AUM fractions from each species were resolved on 17% SDS-PAGE, transferred onto nitrocellulose membrane, and incubated at room temperature for 45 min with 3% bovine serum albumin (Sigma) in TBST (50 mM Tris-Cl, pH 7.4, 150 mM NaCl, 0.05% Tween 20) followed by incubation with biotinylated FimH/C (1 μg/ml) for 1 h at room temperature. The biotinylated FimH/C proteins were visualized using horseradish peroxidase-labeled streptavidin (Sigma) and SuperSignal enhanced chemiluminescent substrate (Pierce).

Gel Electrophoresis and Protein Staining/Destaining—The purified AUM was resolved on 16% tris-glycine polyacrylamide gel (Invitrogen) using an E 19001-Xcell II Mini-Cell (Genisphere Inc., PA) at 125 V constant voltage. Proteins were visualized by GelCode Blue Stain reagent (Pierce) followed by destaining with distilled water. Individual protein bands of interest were excised from the gel.

Protein Reduction and Alkylation—The excised gel bands were cut into pieces of about 1 mm^3 and washed with 50 mM NH_4HCO_3, then 100% acetonitrile (CH_3CN). After removal of the supernatant, gel segments were dried in a Savant Instruments SC 110 SpeedVac™ concentrator (Farmingdale, NY) and incubated at 56 °C for 60 min in 25 μl of 10 mM dithiothreitol in 50 mM NH_4HCO_3. After cooling to room temperature and removal of the supernatant, the gel pieces were incubated at 45 °C for 45 min in the dark in 25 μl of 50 mM fresh iodoacetamide in 50 mM NH_4HCO_3, washed in 50 μl of 50 mM NH_4HCO_3, then 100% CH_3CN, and dried using a SpeedVac to remove SDS, reducing, and alkylation reagents.

In Situ Glycosidase and Protease Digestions—The dried gel pieces were sequentially treated with PNGase F (500 units/ml in 25 mM NH_4HCO_3) and with trypsin (20 ng/μl in 25 mM NH_4HCO_3). For each digestion, the volume of enzyme solution was adjusted to cover the gel pieces, more buffer (50 mM NH_4HCO_3) was added, and the tubes were incubated at 37 °C overnight.

Oligosaccharides and Peptides Extraction—Glycans were extracted from the gel pieces by removing the incubation buffer, which already may have contained some sugars, and using three exchanges of 100 μl water, with sonication for 30 min each time. All supernatants were combined and dried in a SpeedVac. Similarly, peptides were extracted from the gel pieces by removing the incubation buffer, which already may have contained some peptides, and using three changes of 100 μl of

50% acetonitrile in water with sonication for 30 min each time. All extracts were combined and dried in a SpeedVac.

Permethylation of Oligosaccharide—Released glycans were dissolved in Me_2SO and per-*O*-methylated by treating with powdered sodium hydroxide with methyl iodide using the method introduced by Ciucanu and Kerek (39) as modified by Ciucanu and Costello (40).

Mass Spectrometry—Mass spectra were acquired on a Bruker Reflex IV MALDI-TOF MS equipped with a Laser Science nitrogen laser (Franklin, MA) having a 3-ns pulse width at 337 nm or an electrospray ionization (ESI) QSTAR Pulsar *i* quadrupole-orthogonal TOF mass spectrometer (MS and MS/MS) (Applied Biosystems, Foster City, CA).

MALDI-TOF MS—Dried permethylated glycans were dissolved in acetonitrile:water (70:30, v/v). One μl of sample was then mixed with 1 μl of the MALDI matrix 2,5-dihydroxybenzoic acid (10 mg/ml in acetonitrile:water:trifluoroacetic acid (50/50/0.1 v/v/v)), spotted onto the MALDI target plate, allowed to dry and analyzed in the positive reflectron mode with delayed extraction. Permethylated oligosaccharides were observed as $[M+Na]^+$ ions. Zip-Tip^{TM}-cleaned tryptic peptides were dissolved in acetonitrile:water:trifluoroacetic acid (30:70:0.1, v/v/v). One μl of sample solution was mixed with the MALDI matrix α-cyano-4-hydroxycinnamic acid (10 mg/ml in acetonitrile:water:trifluoroacetic acid (50/50/0.1 v/v/v)), deposited on a MALDI target, and observed as $[M+H]^+$ in the positive ion spectra.

ESI Quadrupole-orthogonal TOF MS and Collision-induced Decomposition MS/MS—ESI MS/MS has been a particularly useful tool for the analysis of oligosaccharides, because it provides composition and sequence information based on comparison of fragments (41–43). The solution of permethylated glycans 5 μl in 25 mM NaOH, 50% methanol (60/40, v/v) was loaded into a nanospray tip, and the sample was nanosprayed into the mass spectrometer by increasing the capillary potential slowly until a stable ion current was observed in the positive ion mode. In ESI, the permethylated oligosaccharides gave abundant $[M+n\mathrm{Na}]^{n+}$ ions, and the entire isotopic cluster was selected for the collision-induced decomposition MS/MS analysis (44). Collision-induced decomposition MS/MS spectra were acquired at 30–60 V collision cell voltage, and the resulting spectra were examined manually. Peptides cleaned by Zip-Tip^{TM} were eluted with acetonitrile:water:formic acid (50/50/0.5, v/v/v) and analyzed. Peaks whose observed mass suggested that they contained potential glycosylation sites were selected for MS/MS analyses.

RESULTS

Strategies for Determining the Oligosaccharide Structures of Uroplakins Ia and Ib—Highly purified mouse urothelial plaques contain four major protein subunits, uroplakins Ia (~27 kDa), Ib (29 kDa), II (15 kDa), and IIIa (47 kDa; Fig. 1*A*, *lane 2*). Although UPIa could be quantitatively converted to a lower M_r (deglycosylated) form by Endo H (Fig. 1*B*, *lanes 4* and *5*), only about 30–40% of the UPIb glycans were Endo H-sensitive, and the rest of the glycoprotein required PNGase F for complete deglycosylation (Fig. 1*B*, *lanes 10–12*). Similar results were obtained with bovine uroplakins Ia and Ib, which were only partially resolved by SDS-PAGE (Fig. 1*A*, *lane 3*), although they could be clearly distinguished by immunoblotting using monospecific antibodies; in this case 100% of UPIa (Fig. 1*B*, *lanes 1* and *2*) and 70–80% of the UPIb were Endo H-sensitive (*lanes 7* and *8*). The minimal requirement for Endo H sensitivity is the presence of Manα1–3Manα1–6Manβ1–4GlcNAcβ1–4GlcNAc-. This means that only high mannose and hybrid-type glycans will be released (45, 46). The partial Endo H-sensitivity of UPIb was confusing as this was not entirely consistent with the observation that recombinant FimH binds exclusively to mouse UPIa, with no detectable binding to UPIb (33). To address this problem we devised a strategy to determine the carbohydrate structures of mouse UPIa and UPIb (Fig. 1*C*). Uroplakins were resolved by SDS-PAGE and detected by Coomassie Blue staining (Fig. 1*A*). Bands of interest were then excised and deglycosylated in-gel by treatment with PNGase F. The extracted glycans were subjected to permethylation and then analyzed

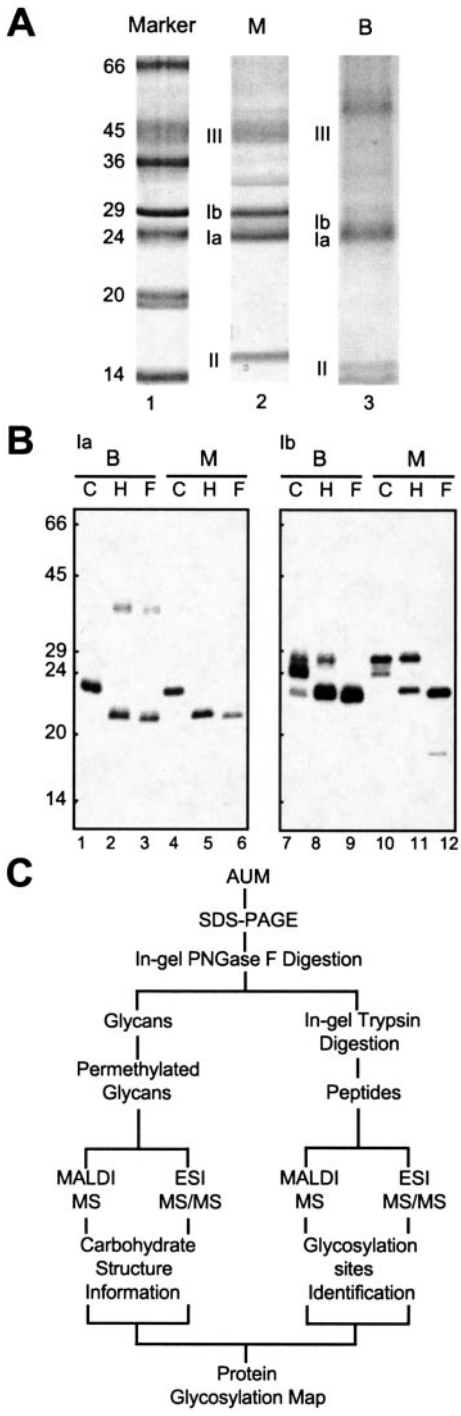

FIGURE 1. **Determination of the glycan structure of uroplakins Ia and Ib.** *A*, separation of mouse (*M*) and bovine (*B*) UPs by SDS-PAGE. *Numbers* on the *left* denote molecular weight of markers. *B*, the endoglycosidase sensitivities of bovine and murine UPIa and UPIb. Bovine (*B*) and mouse (*M*) urothelial plaques were dissolved in SDS, incubated with buffer alone (controls (*C*)), Endo H (*H*), or PNGase F (*F*), resolved by SDS-PAGE, and immunoblotted using antibodies to UPIa or UPIb. *C*, strategies for determining the oligosaccharide structures of electrophoretically purified uroplakins (pathway I) and the identification of the *N*-glycosylation site on the protein backbone (pathway II).

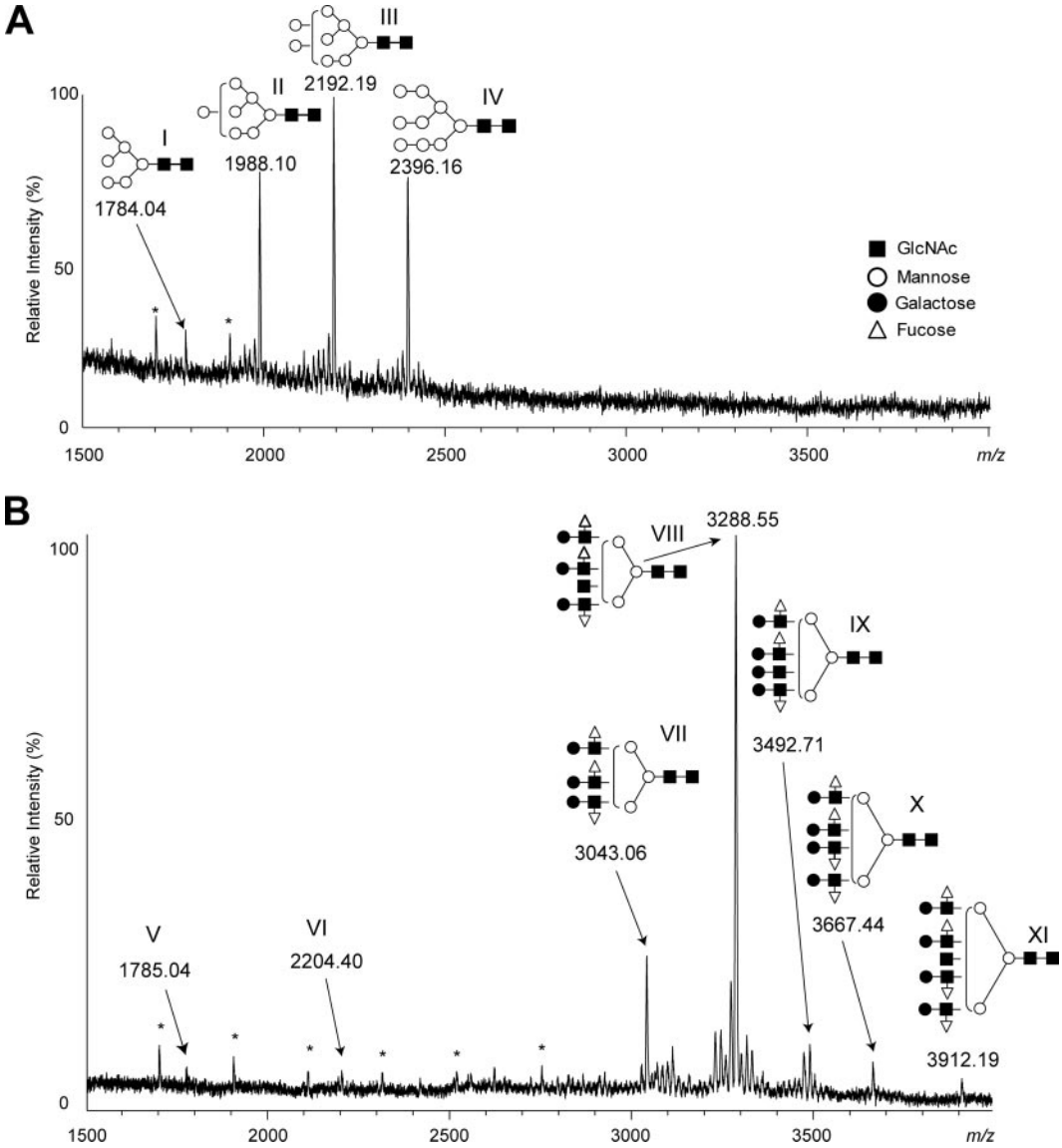

FIGURE 2. **Analysis of the enzymatically released and permethylated glycans from murine UP Ia (*A*) and UP Ib (*B*) by MALDI-TOF MS.** Monoisotopic peaks in *A* and average peaks in *B* are annotated. The structural assignments, as represented by shorthand symbolic notations (*I–XI*), were deduced from their observed mass, their glycosidic, cross-ring fragmentation patterns derived from ESI MS/MS, and the normal *N*-linked glycan structure, except for glycan V and VI, since no ESI MS/MS could be obtained due to the low abundance of the glycoforms. *, polyhexose contaminants.

by MALDI-TOF MS and by ESI MS/MS. After release of the *N*-glycans, the deglycosylated proteins remaining in the gel were trypsin-digested. The products from the proteolysis were analyzed by MALDI MS and ESI MS/MS to identify the glycan-released peptides and locate the previously occupied glycosylation sites.

Mouse Uroplakin Ia and Ib Harbor Mainly High Mannose and Complex Glycans, Respectively—When the glycans released from mouse UPIa were permethylated and analyzed by MALDI-TOF MS, multiple peaks were observed whose *m*/*z* values were spaced at intervals of 204.1 ± 0.1 (calculated monoisotopic mass of a permethylated Hex residue, 204.100 atomic mass units), suggesting the presence of a glycan series with differing numbers of hexoses (Fig. 2*A*). The oligosaccharide structures of all the major monoisotopic peaks were deduced from their observed mass, and their glycosidic and cross-ring fragmentation patterns were derived from ESI MS/MS and the normal *N*-linked glycan structure. Fig. 3*A* presents a representative MS/MS spectrum that was assigned to glycoform IV, $Man_9GlcNAc_2$. Designations of fragments are based on the accepted nomenclature for oligosaccharide fragmentation introduced by Domon and Costello, shown in supplemental Fig. 1 (47). The prominent fragment ions B and Y observed indicated that these glycans possess hexoses as non-reducing termini (please see supplemental Figs. 3, 5, and 6 for the interpretation of other high mannose glycans). Moreover, since the ratios of signal intensities (from individual glycans greater than 1 kDa irrespective of their structures) are known to be semiquantitative in MALDI-TOF mass spectra, we could use these data to estimate the relative abundances of the various components (48, 49). This information as well as the observed and calculated masses and the proposed compositions of various glycoforms are summarized in Table 1. Finally, the occupancy of the potential *N*-glycosylation site at Asn-169 was mapped by the identification by MALDI-TOF MS of a single tryptic peptide (residues 152–175) that had undergone the expected Asn-169 to Asp-169 conversion upon deglycosylation (Fig. 4*A*, supplemental Fig. 2). The sequence of this peptide was confirmed by ESI MS/MS (data not shown); this result was consistent with our previous investigation of mouse UPIa using ^{18}O labeling and tandem mass spectrometry (33).

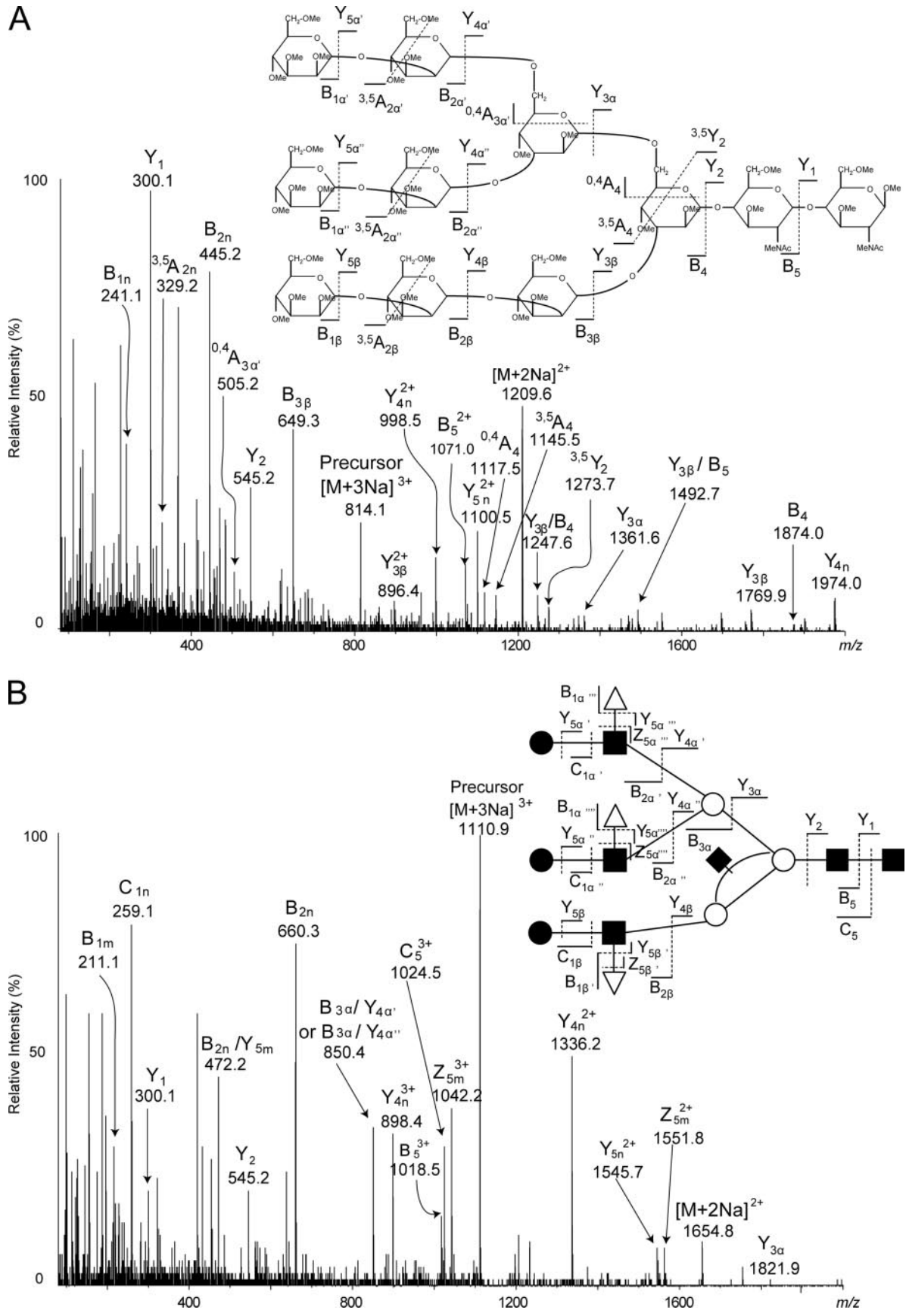

FIGURE 3. **Analysis by ESI MS/MS of permethylated glycan ions at *m/z* 814.1 (3+) (*A*), corresponding to structure IV of murine UPIa, and *m/z* 1110.9 (3+), corresponding to structure VIII of UPIb (*B*).** The illustrated glycan structures were derived from the MS/MS fragmentation patterns. Monoisotopic peaks are annotated, and the assignment of peaks takes into account the normal *N*-glycan structures. All fragments contain sodium. $n = \alpha', \alpha'', \beta$; $m = \alpha''', \alpha'''', \beta'$.

TABLE 1

Proposed compositions of the released and permethylated glycans from in-gel PNGase F digestion of murine UP Ia and UP Ib, respectively

Compositions were tentatively assigned to MALDI-TOF MS peaks on the basis of *m/z* values and confirmed by ESI MS/MS. Mon, monoisotopic mass of the $[M+Na]^+$ ion of the glycans. Avg, average mass of the $[M+Na]^+$ ion of the glycans.

Murine UP Ia	Observed $[M+Na]^+$ (Mon)	Calculated $[M + Na]^+$ (Mon)	Proposed composition	% Total glycoform
I	1784.04	1783.88	$HexNAc_2Hex_6$	5
II	1988.10	1987.98	$HexNAc_2Hex_7$	28
III	2192.19	2192.08	$HexNAc_2Hex_8$	43
IV	2396.16	2396.18	$HexNAc_2Hex_9$	24
Murine UP Ib	**Observed $[M+Na]^+$ (Avg)**	**Calculated $[M + Na]^+$ (Avg)**	**Proposed composition**	**% Total glycoform**
V	1785.04	1784.95	$HexNAc_2Hex_6$	6
VI	2204.40	2204.42	$HexNAc_2Hex_5$[HexNAcHexDeoxyHex]	6
VII	3043.06	3043.37	$[HexNAc_2Hex_3][HexNAcHexDeoxyHex]_3$	14
VIII	3288.55	3288.64	$[HexNAc_2Hex_3][HexNAcHexDeoxyHex]_3HexNAc$	54
IX	3492.71	3492.86	$[HexNAc_2Hex_3][HexNAcHexDeoxyHex]_3HexNAcHex$	8
X	3667.44	3667.06	$[HexNAc_2Hex_3][HexNAcHexDeoxyHex]_4$	7
XI	3912.19	3912.34	$[HexNAc_2Hex_3][HexNAcHexDeoxyHex]_4HexNAc$	5

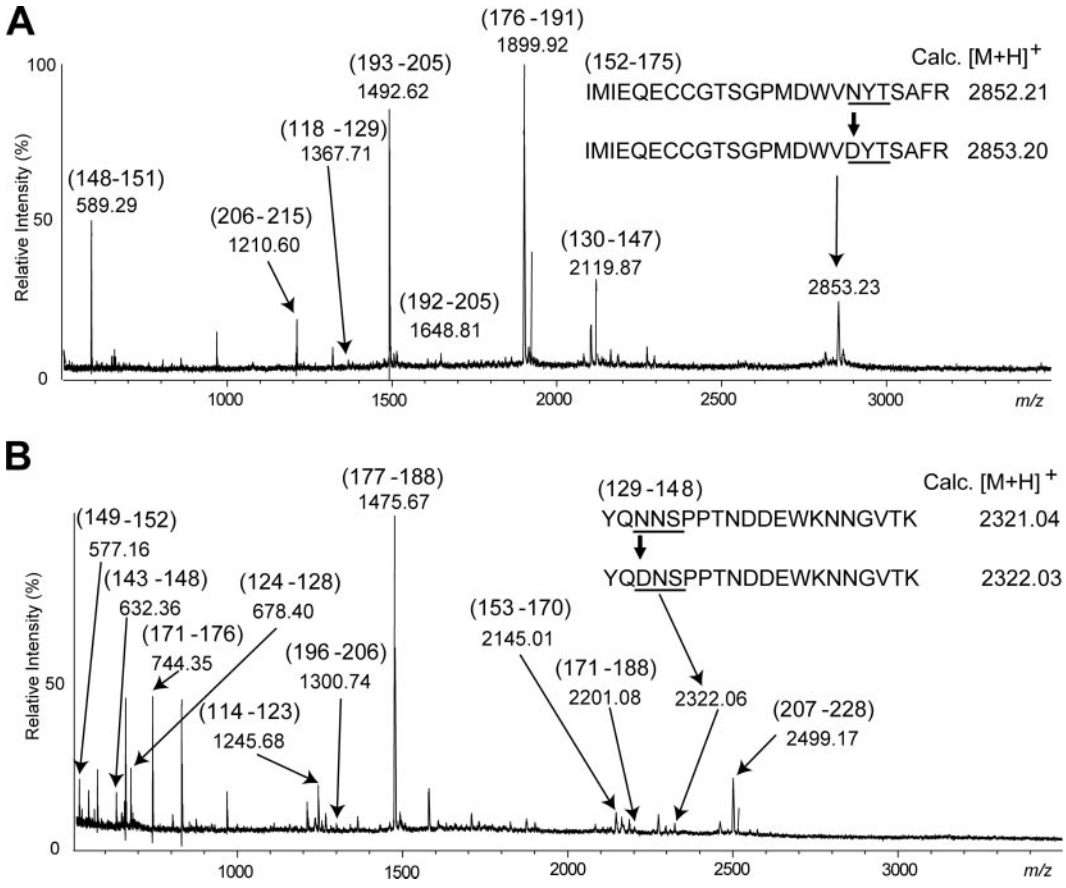

FIGURE 4. **Analysis by MALDI-TOF MS of the tryptic peptides of murine UPIa (*A*) and UPIb (*B*) after deglycosylation.** The peaks at *m/z* 2853.23 and 2322.06 correspond to the initially glycosylated peptides that have undergone glycan loss and Asn to Asp conversion in their *N*-glycosylation motifs (*underlined*), as shown in the schemes. The peptide sequences were established based on the observed b- and y-series ions in the ESI MS/MS analysis (data not shown). The *numbers* in *parenthesis* designate amino acid intervals in UPIa and -Ib.

Similar analyses were performed on SDS-PAGE-purified mouse UPIb, which were found to contain a series of high mannose, hybrid, and multiple-antennary complex glycans (Fig. 2*B*). The peaks at *m/z* 1785.04 and 2204.40 were consistent with high mannose and hybrid *N*-glycans, whereas those at *m/z* 3043.06, 3288.55, 3492.71, 3667.44, and 3912.19 corresponded to a series of complex glycans (see Table 1 for the observed and calculated masses as well as the proposed compositions of UPIb-associated glycoforms V to XI). Assignments of the sequences of the glycans were based on the results from collision-induced decomposition tandem mass spectrometry (see Fig. 3*B* for a representative tandem MS experiment on glycoform VIII). The particularly abundant ion at *m/z* 660.3 (the singly sodiated $B_{2\alpha'}$ ion (or $B_{2\alpha''}$, or $B_{2\beta}$)) supported the presence of an antenna unit composed of a GlcNAc, a Gal, and a Fuc residue; observations of the doubly charged ion at *m/z* 1336.2 led to its assignment as the fragment $Y_{4\alpha'}$ ion (or $Y_{4\alpha''}$, or $Y_{4\beta}$) implying the loss of this antenna unit, as mentioned above. In addition, C_{1n} and Y_{5m}/B_{2n} observed at *m/z* 259.1 and 472.2 indicate that the Fuc can only be attached to a HexNAc residue, not the terminal Gal at the non-reducing end. Furthermore, the deduced structures have only unsubstituted GlcNAc residues at the reducing terminus, *i.e.* there is no "core fucosylation." These results indicated that the mouse UPIb-associated glycans were predominantly (>85%) of the complex type (structures VII to XI as shown in Fig. 2*B* and Table 1) with less than 15% of high mannose (**V**) and hybrid glycans (**VI**). In-gel tryptic digestion of the deglycosylated

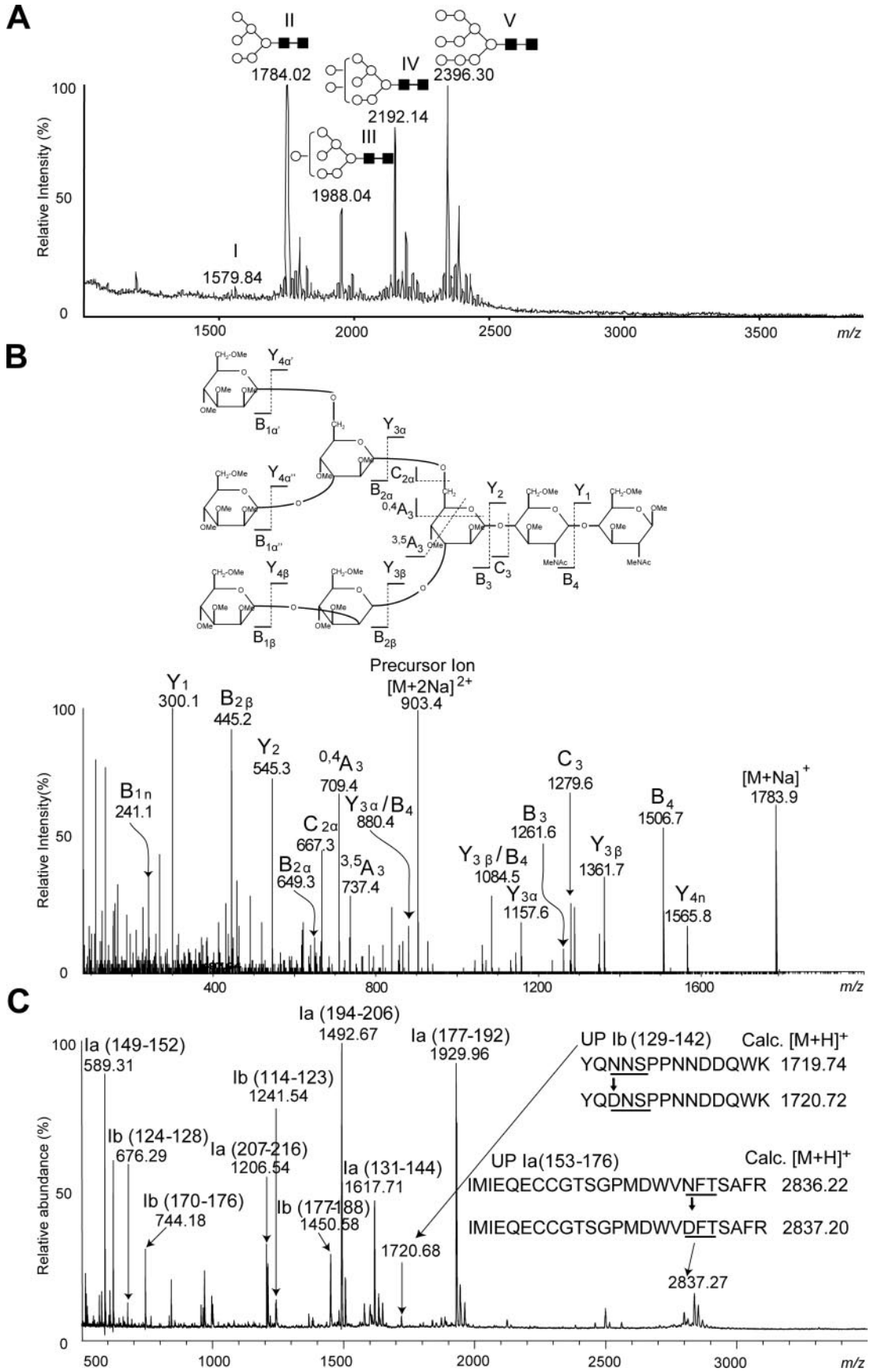

FIGURE 5. **Determination of the sequence and anchoring site of the bovine UPIa/UPIb glycans.** *A*, analysis of the permethylated glycans from a mixture of bovine UPIa and UPIb by MALDI-TOF MS. A mixture of bovine UPIa and -Ib was used for this analysis because they are not as well separated electrophoretically as the mouse analogues. The assumed structures, as shown, were verified by ESI MS/MS (Fig. 5*B*, supplemental Figs. 4–6) and are summarized in Table 2, except for glycan I, since no ESI MS/MS was obtained due to the low

TABLE 2

Proposed compositions of the released and permethylated glycans from in-gel PNGase F digestion of bovine UP Ia and UP Ib mixture

Compositions were tentatively assigned to MALDI MS peaks on the basis of *m/z* values and confirmed by ESI MS/MS. Mon, monoisotopic mass of the $[M+Na]^+$ ion of the glycans.

Bovine UP Ia/Ib	Observed $[M+Na]^+$ (Mon)	Calculated $[M+Na]^+$ (Mon)	Proposed composition	% Total glycoform
I	1579.84	1579.78	$HexNAc_2Hex_5$	4
II	1784.02	1783.88	$HexNAc_2Hex_6$	43
III	1988.04	1987.98	$HexNAc_2Hex_7$	11
IV	2192.14	2192.08	$HexNAc_2Hex_8$	20
V	2396.30	2396.18	$HexNAc_2Hex_9$	22

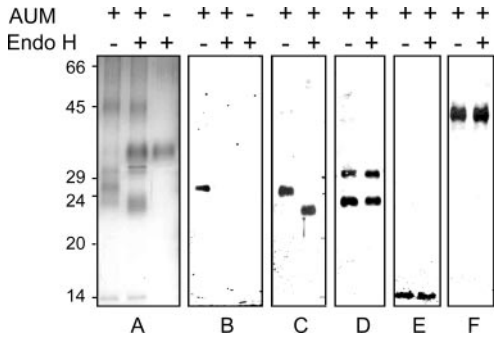

FIGURE 6. **Identification of human UPIa as a major FimH receptor.** Urothelial plaques were isolated from the bladder of human embryo, resolved by SDS-PAGE, and stained with silver nitrate (*A*) or transferred electrophoretically to nitrocellulose and incubated with biotinylated, recombinant FimH·FimC complex (*B*) or immunoblotted with mono-specific antibodies to UP Ia (*C*), UPIb (*D*), UPII (*E*), or UPIIIa (*F*). The ~35-kDa band in the last lane of *panel A* and *B* is Endo H. Note that Endo H reduced the size of UPIa (from 25 to ~22 kDa) but not those of UPIb (two bands remained at 30 and 23 kDa), UPIII (remained at ~45 kDa), or UPII (remained at ~14 kDa) and that the selective binding of FimH to human UPIa is sensitive to Endo H treatment.

protein followed by MALDI MS and ESI tandem MS analyses identified Asn-131 as the previously occupied, *N*-glycosylation site for mouse UPIb (Fig. 4*B*, supplemental Fig. 2).

Bovine UP Ia/Ib Mixture Contains Mainly High Mannose Glycans—As mentioned earlier, bovine UPIa and -Ib could only be partially resolved by SDS-PAGE (Fig. 1*A*, *lane 3*). Therefore, we analyzed the glycans of a mixture of bovine UPIa and -Ib. We found by MALDI-TOF MS (Fig. 5*A*) and ESI MS/MS (Fig. 5*B*, supplemental Figs. 4–6) analyses that the glycans of bovine UPIa/Ib were predominantly high mannose glycans carrying from 5 to 9 mannose residues (Table 2). Analyses of the tryptic peptides from PNGase F-deglycosylated bovine UPIa/Ib established that Asn-170 in UPIa and Asn-131 in UPIb were the occupied *N*-glycosylation sites (Fig. 5*C*, supplemental Fig. 2).

FimH Binds to Human Uroplakin Ia—The finding that the type-1 fimbriated *E. coli* binds selectively to mouse UPIa but probably to both bovine UPIa and -Ib raised the question of which human uroplakin(s) might serve as the FimH receptor (27, 33). We, therefore, tested the FimH binding capacity of the individual uroplakins of the detergent-insoluble urothelial plaques isolated from the bladder urothelia of 16–18-week human embryos using the gel-overlay assay. The four major human uroplakins (the 26-kDa UPIa, 30-kDa UPIb, 14-kDa UPII, and 47-kDa UPIIIa) were well resolved (Fig. 6, *C–F*). The result indicated that 100% of human UPIa was Endo H-sensitive (Fig. 6*C*). However, unlike the murine and bovine UPIb, which were 40 and 80% Endo H-sensitive, respectively, the glycosylated form of human UPIb was completely resistant to Endo H and, therefore, contains 100% complex glycans (Fig. 6*D*). Recombinant FimH was found to bind exclusively UPIa (Fig. 6*B*, *lane 1*), and this binding could be abolished completely by Endo H treatment indicating that the binding was high mannose glycan-dependent (Fig. 6*B*, *second lane*).

DISCUSSION

Differential Glycosylation of Mouse UPIa and UPIb Confers Different Binding to FimH—By determining the oligosaccharide structures of mouse UPIa and -Ib, we now better understand why FimH binds drastically differently to the two closely related mouse glycoproteins, UPIa and UPIb (33). Although the single *N*-glycosylation sites of both mouse UPIa (Asn-169) and UPIb (Asn-131) are modified by *N*-linked glycans, the structures of the glycans differ considerably (Figs. 2 and 3). Mouse UPIa contains a series of high mannose glycans ranging from $Man_6GlcNAc_2$ to $Man_9GlcNAc_2$ with the glycoform distributions indicated in Fig. 2*A* and Table 1. This is consistent with the fact that the *N*-glycans of mouse UPIa can be efficiently removed by Endo H, a glycosidase specific for high mannose glycans (Fig. 1*B*, *lane 5*). Mouse UPIb, however, contains mainly a series of multiple-antennary complex glycans, with a relatively low percentage of hybrid and high mannose glycans (Fig. 2*B* and Table 1). The terminal monosaccharides of mouse UPIb deduced from MS/MS spectra consist of non-mannose moieties including HexNAc (likely GlcNAc), dHex (likely Fuc), and Hex (likely Gal) (Figs. 2*B* and 3*B*). The abundance of terminally exposed mannoses in mouse UPIa and the low content of the same in UPIb clearly explains why FimH lectin-adhesin, whose carbohydrate binding pocket can accommodate only a single mannose (8, 9, 50), binds UPIa but not UPIb at all (31, 33). Although mouse UPIb still retains core mannoses, these residues are deeply embedded and are, thus, unavailable for FimH binding. This observation is of course consistent with the fact that UPIIIa, which harbors complex-type glycans, cannot serve as a receptor for FimH (23, 27).

Although all glycoforms of UPIa high mannose oligosaccharides ($Man_{6-9}GlcNAc_2$) contain terminal mannose residues, it remains unclear whether some glycoforms bind to FimH preferentially. Co-crystallization studies using FimH and mono-mannose offer little insight on how different glycoforms of natural oligosaccharides might interact with FimH (8, 9). *In vitro* binding assays using different substrata also have yielded conflicting results. For instance, type 1-fimbriated *E. coli* appeared to bind pig Tamm-Horsfall protein (THP) in much greater numbers than human THP (51). Because the former has a much higher ratio of $Man_5GlcNAc_2$ to $Man_6GlcNAc_2$ than the latter, although we cannot be certain from the present data, it has been suggested that the 1,3-mannose residue from the trimannosyl core within the $Man_5GlcNAc_2Asn$ is crucial for the high affinity binding between the high mannose chain and FimH (51–55). An additional mannose on top of this FimH binding mannose core, as in the case of $Man_6GlcNAc_2$, could cause steric hindrance, thus, reducing FimH binding. Such a preference for shorter mannose chain is not shared by all bacteria; for example, a FimH-like adhesin expressed by an intestinal

abundance of this glycoform. *B*, determination of the bovine UPIa/Ib glycan structures. Shown is the ESI MS/MS spectrum of permethylated glycan ions at *m/z* 903.4 (2+), corresponding to structure II in *panel A* from bovine UP Ia/Ib. The illustrated structure was derived from the MS/MS fragmentation pattern and was the dominant isomer for the glycan. For example, the abundant peaks at *m/z* 709.4, 737.4, and 880.4 are characteristic fragments that only occur for the isomer shown in the *upper panel* of Fig. 5*B*. Monoisotopic peaks are annotated, and the assignment of peaks is based on the normal *N*-glycan structures. All fragments contain sodium. $n = \alpha', \alpha'', \beta$. *C*, identification of the *N*-glycosylated bovine UPIa/Ib peptide. The MALDI-TOF MS spectrum of the deglycosylated tryptic peptides of bovine UP Ia/Ib. The peaks at *m/z* 2837.27 and 1720.68 correspond to the $[M+H]^+$ form of the bovine UPIa and UPIb peptides harboring *N*-glycosylation motifs (*underlined*). The enzymatic release of their *N*-linked glycans converts Asn (*N*) to Asp (*D*). The *numbers* in *parenthesis* designate amino acid intervals in UPIa and -Ib.

E. coli prefers the longest high mannose chain ($Man_9GlcNAc_2$) over shorter chains (56). It should be noted that mouse UPIa contains only a very small amount of $Man_6GlcNAc_2$. Assuming that the longer mannose chains, such as the $Man_{7-9}GlcNAc_2$ are poorer FimH substrates than the shorter glycans suggests that the UPIa is a weak and, thus, perhaps not an "optimal" receptor for the pathogenic *E. coli*. Whether the host evolved such a suboptimal receptor as a host defense mechanism, reflecting an ongoing warfare between the host and the type 1-fimbriated *E. coli*, remains to be seen. Clearly needed are further studies to determine *e.g.* the binding of recombinant FimH to specific spots on glycan arrays can quantitatively measure the binding of FimH to different length high mannose chains. Alternatively, FimH can be used to fish out from a mixture of natural high mannose oligosaccharides the best binder(s). Eventually, co-crystallization experiments using FimH and natural high mannose oligosaccharides will have to be carried out to ascertain not only which terminal mannose binds to the FimH binding pocket but also how other terminal and branched mannoses affect the binding.

Although the glycan structures of mouse UPIa and UPIb as derived from the mass spectrometric data are completely consistent with and can account for the FimH binding data, the interpretation of the Endo H sensitivities of the two mouse uroplakins is not straightforward. It has been reported that Endo H cleaves high mannose and "hybrid" glycans; this stated specificity is not consistent with our finding, however, that the protein in the mouse UPIb band we have analyzed by mass spectrometry contains almost exclusively complex glycans (Fig. 2*B*). The explanation may be simply that the UPIb proteins bearing the different glycoforms are slightly resolved on the gel and the region of the major UPIb band cut out for MS analysis contained predominantly the complex glycoforms (Fig. 1*B*, *lane 10*), whereas the minor UPIb protein with high mannose glycoforms migrated closer to the position of the UPIa band, as seen in Fig. 1*B* (*lanes 4* and *10*).

Structural and Partnership Constraints May Contribute to Differences in UPIa and UPIb Glycosylation—The fact that mouse UPIa and UPIb bear very different sugar moieties was somewhat unexpected because these two proteins are highly similar in many respects. The two proteins are ~40% identical in amino acid sequence, and both possess four transmembrane domains (TM) with a large extracellular loop (connecting the third and the fourth TMs), where the single glycosylation site resides (20). Both proteins belong to an expanding family of tetraspanins that play important and diverse roles in growth, differentiation, signal transduction, and tumorigenesis (20, 57–60). Our current study indicates clearly, however, that UPIa and UPIb are processed quite differently with regard to their glycan formation (Figs. 2 and 3). It has been well established that the initial step of *N*-glycosylation, a co-translational process identical for all proteins, involves the transfer of an *N*-glycan precursor ($Glc_3Man_9GlcNAc_2$) from lipid-linked dolichol to a protein glycosylation site (61–63). The subsequent trimming of the precursor by α-mannosidases in the endoplasmic reticulum and addition of other sugar moieties by glycosyltransferases in the Golgi complex can vary significantly depending on peptide folding and accessibility of the glycosylation sites to glycosylating enzymes (62, 64). It is possible that the accessibilities of the glycans of UPIa and UPIb to sugar-modifying enzymes in the endoplasmic reticulum and Golgi are intrinsically different due to differences in their amino acid sequences (about 60% of amino acid divergence) (20). On the other hand, we have shown recently that the conformation of intact pro-UPII undergoes drastic changes upon the enzymatic removal of its prosequence by furin in the trans-Golgi network (59). Therefore, an alternative and perhaps more attractive interpretation is that the prosequence portion of pro-UPII upon binding to its partner UPIa in the endoplasmic reticulum can block UPIa's single glycan from further trimming by the sugar-modifying enzymes. This blockage of the UPIa glycan by pro-UPII is apparently transient in nature, however, since the glycan of mature UPIa, when it reaches the apical urothelial plaques, becomes fully accessible to Endo H digestion, possibly related to the furin removal of the prosequence of UPII.[4] Site-directed mutagenesis and domain swapping studies are needed to determine how peptide folding and heterodimerization affect the glycosylation of UPIa and UPIb.

We have observed that bovine UPIa/Ib contains mainly high mannose glycans. It may represent an exception to the rule, perhaps because of early stage differences in the binding to its partner. Unlike mouse UPIb and human UPIb, which on a gel are well resolved from UPIa and can be shown to contain complex-type glycans, it has been a major technical challenge to discern the oligosaccharide structure of bovine UPIb because it can be hardly separated from bovine UPIa on SDS-PAGE (Fig. 1*A*, *lane 3*) (21, 24). Our earlier gel-overlay assay using radiolabeled, type 1-fimbriated *E. coli* on SDS-PAGE-separated bovine uroplakins appeared to detect two bands, one clearly corresponding to bovine UPIa and another slightly above UPIa, which we attributed to UPIb binding (27). Endo H treatment followed by SDS-PAGE and immunoblotting indicated that about 80% of the UPIb was Endo H-sensitive, whereas the remaining was Endo H-resistant (20, 24) (Fig. 1*B*, *lane 11*). These results were interpreted to mean that bovine UPIb contains both high mannose and complex-type glycans. Our current study of *N*-linked (PNGase F-treated) glycans released from a mixture of bovine UPIa and UPIb failed, however, to detect a significant amount of complex glycans, suggesting that bovine UPIb is primarily modified by high mannose glycans. Therefore, it remains possible that in cattle both UPIa and -Ib can interact with FimH and be the urothelial receptors for type 1-fimbriated *E. coli*.

The results obtained by overlay assays before and after glycosidase treatments of human UPIa and -Ib indicate that the UPIa glycans are exclusively high mannose structures and UPIb has only complex glycans. Although insufficient material was available to allow MS analysis, our data strongly suggest that in humans the type 1-fimbriated *E. coli* binds exclusively to UPIa.

Biological and Clinical Implications—Based on the data presented here and those shown earlier, we can conclude that the unmodified, terminally exposed mannoses of UPIa are the main urothelial receptors for FimH lectin adhesin of the type 1-fimbriated *E. coli*, although we cannot rule out the possibility that in some species UPIb may harbor some high mannose glycans, thus, also contributing to some degree bacterial binding. These receptors are remarkably conserved in all species studied to date, including mouse (33), cattle (27), and human (Fig. 6), implicating a critical role by these receptors in urinary tract infection pathogenesis. As mentioned earlier, within the type 1-fimbriated *E. coli* strains, phenotypic variants have evolved that exhibit enhanced affinity to the terminal mannose residues (32, 65). Interestingly, these variants are uncommon in the fecal flora but are predominant in the urinary tract infection isolates, perhaps reflecting a tissue tropism by these variants for the urinary tract niche (32). The expression of highly conserved terminal mannoses by UPIa may explain at least in part why such monomannose binding *E. coli* strains have a selective advantage for the urinary tract.

The proven importance of the terminal mannoses of UPIa in *E. coli* adhesion also implies that the changing status of UPIa glycosylation or that of other urothelial surface proteins may alter the host susceptibility to urinary tract infections. There are ample examples that, in certain

[4] G. Zhou, unpublished observation.

disease states, protein glycosylation patterns can change (66). It is of interest to note in a recent study that FimH-expressing *E. coli* appeared to bind better to urothelial cells obtained from diabetic patients than those from healthy individuals (67). Whether this can be attributed to altered uroplakin glycosylation is unknown, but it certainly deserves further investigation.

As has been recently demonstrated, the interaction of FimH with terminally exposed mannose residues on UPIa can lead to severe consequences to host urothelial cells including internalization of the bacteria into the superficial umbrella cells (28). Once inside the cells, the bacteria can propagate rapidly, forming intracellular biofilms that are highly resistant to the antibiotics (29). Some of the intracellular bacteria can stay dormant for an extended period of time before breaking out and serving as seeds for a new round of infection (29). A logical means to prevent these serious consequences from taking place from the start would be to block the FimH from binding to the UPIa receptors using high mannose mimetic inhibitors. Information obtained from this study should help the rational design of such inhibitory molecules.

Acknowledgments—We thank Drs. Ulf Sommer, Robert Seward, Joseph Zaia, John F. Cipollo, Peter B. O'Connor (all of Boston University School of Medicine), Huaibin Wang, Fang-Ming Deng, Andrew Hu, and Seung-Sup Kim (New York University School of Medicine) for valuable suggestions and help. We particularly thank R. Glockshuber (Universität Zurich) for the plasmid ll and George Georgiou (University of Texas at Austin) for the bacterial strain for the production of the recombinant FimH·FimC complex.

REFERENCES

1. Hasty, D. L., Wu, X.-R., Dykuizen, D. E., and Sokurenko, E. V. (2005) in *Colonization of Mucosal Surfaces* (Nataro, J. P., Cohen, P. S., Mobley, H. L. T., and Weiser, J. N., eds) Vol. 24, pp. 351–377, American Society for Microbiology Press, Washington, D.C.
2. Abraham, S. N., Sun, D., Dale, J. B., and Beachey, E. H. (1988) *Nature* **336,** 682–684
3. Connell, I., Agace, W., Klemm, P., Schembri, M., Marild, S., and Svanborg, C. (1996) *Proc. Natl. Acad. Sci. U. S. A.* **93,** 9827–9832
4. Mulvey, M. A., Schilling, J. D., Martinez, J. J., and Hultgren, S. J. (2000) *Proc. Natl. Acad. Sci. U. S. A.* **97,** 8829–8835
5. Schilling, J. D., Mulvey, M. A., and Hultgren, S. J. (2001) *J. Infect. Dis.* **183,** Suppl. 1, 36–40
6. Klemm, P., Schembri, M., and Hasty, D. L. (1996) *Adv. Exp. Med. Biol.* **408,** 193–195
7. Jones, C. H., Pinkner, J. S., Roth, R., Heuser, J., Nicholes, A. V., Abraham, S. N., and Hultgren, S. J. (1995) *Proc. Natl. Acad. Sci. U. S. A.* **92,** 2081–2085
8. Choudhury, D., Thompson, A., Stojanoff, V., Langermann, S., Pinkner, J., Hultgren, S. J., and Knight, S. D. (1999) *Science* **285,** 1061–1066
9. Hung, C. S., Bouckaert, J., Hung, D., Pinkner, J., Widberg, C., DeFusco, A., Auguste, C. G., Strouse, R., Langermann, S., Waksman, G., and Hultgren, S. J. (2002) *Mol. Microbiol.* **44,** 903–915
10. O'Hanley, P., Lark, D., Falkow, S., and Schoolnik, G. (1985) *J. Clin. Investig.* **75,** 347–360
11. Koss, L. G. (1969) *Lab. Investig.* **21,** 154–168
12. Hicks, R. M. (1965) *J. Cell Biol.* **26,** 25–48
13. Walz, T., Haner, M., Wu, X. R., Henn, C., Engel, A., Sun, T. T., and Aebi, U. (1995) *J. Mol. Biol.* **248,** 887–900
14. Kachar, B., Liang, F., Lins, U., Ding, M., Wu, X. R., Stoffler, D., Aebi, U., and Sun, T. T. (1999) *J. Mol. Biol.* **285,** 595–608
15. Min, G., Zhou, G., Schapira, M., Sun, T. T., and Kong, X. P. (2003) *J. Cell Sci.* **116,** 4087–4094
16. Hicks, R. M., and Ketterer, B. (1969) *Nature* **224,** 1304–1305
17. Taylor, K. A., and Robertson, J. D. (1984) *J. Ultrastruct. Res.* **87,** 23–30
18. Oostergetel, G. T., Keegstra, W., and Brisson, A. (2001) *J. Mol. Biol.* **314,** 245–252
19. Yu, J., Manabe, M., Wu, X. R., Xu, C., Surya, B., and Sun, T. T. (1990) *J. Cell Biol.* **111,** 1207–1216
20. Yu, J., Lin, J. H., Wu, X. R., and Sun, T. T. (1994) *J. Cell Biol.* **125,** 171–182
21. Wu, X. R., Manabe, M., Yu, J., and Sun, T. T. (1990) *J. Biol. Chem.* **265,** 19170–19179
22. Lin, J. H., Wu, X. R., Kreibich, G., and Sun, T. T. (1994) *J. Biol. Chem.* **269,** 1775–1784
23. Wu, X. R., and Sun, T. T. (1993) *J. Cell Sci.* **106,** 31–43
24. Wu, X. R., Lin, J. H., Walz, T., Haner, M., Yu, J., Aebi, U., and Sun, T. T. (1994) *J. Biol. Chem.* **269,** 13716–13724
25. Wu, X. R., Medina, J. J., and Sun, T. T. (1995) *J. Biol. Chem.* **270,** 29752–29759
26. Tu, L., Sun, T. T., and Kreibich, G. (2002) *Mol. Biol. Cell* **13,** 4221–4230
27. Wu, X. R., Sun, T. T., and Medina, J. J. (1996) *Proc. Natl. Acad. Sci. U. S. A.* **93,** 9630–9635
28. Mulvey, M. A., Lopez-Boado, Y. S., Wilson, C. L., Roth, R., Parks, W. C., Heuser, J., and Hultgren, S. J. (1998) *Science* **282,** 1494–1497
29. Anderson, G. G., Palermo, J. J., Schilling, J. D., Roth, R., Heuser, J., and Hultgren, S. J. (2003) *Science* **301,** 105–107
30. Martinez, J. J., Mulvey, M. A., Schilling, J. D., Pinkner, J. S., and Hultgren, S. J. (2000) *EMBO J.* **19,** 2803–2812
31. Min, G., Stolz, M., Zhou, G., Liang, F., Sebbel, P., Stoffler, D., Glockshuber, R., Sun, T. T., Aebi, U., and Kong, X. P. (2002) *J. Mol. Biol.* **317,** 697–706
32. Sokurenko, E. V., Chesnokova, V., Dykhuizen, D. E., Ofek, I., Wu, X. R., Krogfelt, K. A., Struve, C., Schembri, M. A., and Hasty, D. L. (1998) *Proc. Natl. Acad. Sci. U. S. A.* **95,** 8922–8926
33. Zhou, G., Mo, W. J., Sebbel, P., Min, G., Neubert, T. A., Glockshuber, R., Wu, X. R., Sun, T. T., and Kong, X. P. (2001) *J. Cell Sci.* **114,** 4095–4103
34. Dell, A., and Morris, H. R. (2001) *Science* **291,** 2351–2356
35. Rudd, P. M., and Dwek, R. A. (1997) *Crit. Rev. Biochem. Mol. Biol.* **32,** 1–100
36. Dwek, R. A., Edge, C. J., Harvey, D. J., Wormald, M. R., and Parekh, R. B. (1993) *Annu. Rev. Biochem.* **62,** 65–100
37. Rudd, P. M., and Dwek, R. A. (1997) *Curr. Opin. Biotechnol.* **8,** 488–497
38. Vetsch, M., Sebbel, P., and Glockshuber, R. (2002) *J. Mol. Biol.* **322,** 827–840
39. Ciucanu, I., and Kerek, F. (1984) *Carbohydr. Res.* **131,** 209–217
40. Ciucanu, I., and Costello, C. E. (2003) *J. Am. Chem. Soc.* **125,** 16213–16219
41. Gillece-Castro, B. L., and Burlingame, A. L. (1990) *Methods Enzymol.* **193,** 689–712
42. Reinhold, V. N., Reinhold, B. B., and Chan, S. (1996) *Methods Enzymol.* **271,** 377–402
43. Richter, W. J., Muller, D. R., and Domon, B. (1990) *Methods Enzymol.* **193,** 607–623
44. Harvey, D. J. (2000) *J. Mass Spectrom.* **35,** 1178–1190
45. Maley, F., Trimble, R. B., Tarentino, A. L., and Plummer, T. H., Jr. (1989) *Anal. Biochem.* **180,** 195–204
46. Trimble, R. B., Tarentino, A. L., Plummer, T. H., Jr., and Maley, F. (1978) *J. Biol. Chem.* **253,** 4508–4511
47. Domon, B., and Costello, C. E. (1988) *Glycoconj. J.* **5,** 397–409
48. Harvey, D. J. (1993) *Rapid Commun. Mass Spectrom.* **7,** 614–619
49. Naven, T. J., and Harvey, D. J. (1996) *Rapid Commun. Mass Spectrom.* **10,** 1361–1366
50. Bouckaert, J., Berglund, J., Schembri, M., De Genst, E., Cools, L., Wuhrer, M., Hung, C. S., Pinkner, J., Slattegard, R., Zavialov, A., Choudhury, D., Langermann, S., Hultgren, S. J., Wyns, L., Klemm, P., Oscarson, S., Knight, S. D., and De Greve, H. (2005) *Mol. Microbiol.* **55,** 441–455
51. Cavallone, D., Malagolini, N., Monti, A., Wu, X. R., and Serafini-Cessi, F. (2004) *J. Biol. Chem.* **279,** 216–222
52. Lindhorst, T. K., Kieburg, C., and Krallmann-Wenzel, U. (1998) *Glycoconj. J.* **15,** 605–613
53. Neeser, J. R., Koellreutter, B., and Wuersch, P. (1986) *Infect. Immun.* **52,** 428–436
54. Firon, N., Ofek, I., and Sharon, N. (1984) *Infect. Immun.* **43,** 1088–1090
55. Sharon, N. (1987) *FEBS Lett.* **217,** 145–157
56. Pan, Y. T., Xu, B., Rice, K., Smith, S., Jackson, R., and Elbein, A. D. (1997) *Infect Immun.* **65,** 4199–4206
57. Hemler, M. E. (2003) *Annu. Rev. Cell Dev. Biol.* **19,** 397–422
58. Maecker, H. T., Todd, S. C., and Levy, S. (1997) *FASEB J.* **11,** 428–442
59. Hu, C. C., Liang, F. X., Zhou, G., Tu, L., Tang, C. H., Zhou, J., Kreibich, G., and Sun, T. T. (2005) *Mol. Biol. Cell* **16,** 3937–3950
60. Boucheix, C., and Rubinstein, E. (2001) *Cell. Mol. Life Sci.* **58,** 1189–1205
61. Kornfeld, R., and Kornfeld, S. (1985) *Annu. Rev. Biochem.* **54,** 631–664
62. Jenkins, N., Parekh, R. B., and James, D. C. (1996) *Nat. Biotechnol.* **14,** 975–981
63. Burda, P., and Aebi, M. (1999) *Biochim. Biophys. Acta* **1426,** 239–257
64. Jones, J., Krag, S. S., and Betenbaugh, M. J. (2005) *Biochim. Biophys. Acta* **1726,** 121–137
65. Sokurenko, E. V., Chesnokova, V., Doyle, R. J., and Hasty, D. L. (1997) *J. Biol. Chem.* **272,** 17880–17886
66. Durand, G., and Seta, N. (2000) *Clin. Chem.* **46,** 795–805
67. Geerlings, S. E., Meiland, R., van Lith, E. C., Brouwer, E. C., Gaastra, W., and Hoepelman, A. I. (2002) *Diabetes Care* **25,** 1405–1409